PROTEINS
STRUCTURE ■ FUNCTION ■ BIOINFORMATICS

Determining the molecular mechanism of inactivation by chemical modification of triosephosphate isomerase from the human parasite *Giardia lamblia*: A study for antiparasitic drug design

Sergio Enríquez-Flores,[1] Adela Rodríguez-Romero,[2] Gloria Hernández-Alcántara,[1] Jesús Oria-Hernández,[1] Pedro Gutiérrez-Castrellón,[1] Gerardo Pérez-Hernández,[3] Ignacio de la Mora-de la Mora,[1] Adriana Castillo-Villanueva,[1] Itzhel García-Torres,[1] Sara T. Méndez,[1] Saúl Gómez-Manzo,[1] Angélica Torres-Arroyo,[1] Gabriel López-Velázquez,[1]* and Horacio Reyes-Vivas[1]*

[1] Laboratorio de Bioquímica-Genética, Torre de Investigación, Instituto Nacional de Pediatría, Secretaría de Salud, 04530, México, D.F
[2] Instituto de Química, Universidad Nacional Autónoma de México, 04510, México, D.F
[3] Departamento de Ciencias Naturales, Universidad Autónoma Metropolitana Cuajimalpa, 01120, México, D.F

ABSTRACT

Giardiasis, the most prevalent intestinal parasitosis in humans, is caused by *Giardia lamblia*. Current drug therapies have adverse effects on the host, and resistant strains against these drugs have been reported, demonstrating an urgent need to design more specific antigiardiasic drugs. ATP production in *G. lamblia* depends mainly on glycolysis; therefore, all enzymes of this pathway have been proposed as potential drug targets. We previously demonstrated that the glycolytic enzyme triosephosphate isomerase from *G. lamblia* (GlTIM), could be completely inactivated by low micromolar concentrations of thiol-reactive compounds, whereas, in the same conditions, the activity of human TIM (HuTIM) was almost unaltered. We found that the chemical modification (derivatization) of at least one Cys, of the five Cys residues per monomer in GlTIM, causes this inactivation. In this study, structural and functional studies were performed to describe the molecular mechanism of GlTIM inactivation by thiol-reactive compounds. We found that the Cys222 derivatization is responsible for GlTIM inactivation; this information is relevant because HuTIM has a Cys residue in an equivalent position (Cys217). GlTIM inactivation is associated with a decrease in ligand affinity, which affects the entropic component of ligand binding. In summary, this work describes a mechanism of inactivation that has not been previously reported for TIMs from other parasites and furthermore, we show that the difference in reactivity between the Cys222 in GlTIM and the Cys217 in HuTIM, indicates that the surrounding environment of each Cys residue has unique structural differences that can be exploited to design specific antigiardiasic drugs.

Proteins 2011; 79:2711–2724.

Key words: triosephosphate isomerase; TIM; *Giardia*; drug design; cysteine derivatization; calorimetry; X-ray crystallography.

INTRODUCTION

Giardia lamblia, the causative agent of giardiasis, is a protozoan with worldwide distribution, which causes ~ 200 million symptomatic cases per year and mainly affects pediatric and immunocompromised persons.[1] Clinical manifestations of acute giardiasis range from asymptomatic carriage to abdominal pain, vomit, and diarrhea, and chronic infection can progress to malabsorption syndrome caused by intestinal damage.[2] Pharmacotherapy against giardiasis involves the use of compounds derived from nitroimidazoles and benzimidazoles[3]; however, there are reservations concerning the application of these compounds, because of the side effects in the host and the emergence of resistant strains to these drugs.[3–5] It is clear that new approaches capable of generating highly specific antigiardiasic drugs are required, and thus, multiple efforts to find new antigiardiasic compounds are currently in progress.[3,6,7]

Additional Supporting Information may be found in the online version of this article.

Grant sponsor: Consejo Nacional de Ciencia y Tecnología (CONACyT, México); Grant numbers: 104841, 62321 and 106126

*Correspondence to: Horacio Reyes-Vivas, Insurgentes Sur 3700-C, Col. Insurgentes Cuicuilco. México, D.F. CP 04530. E-mail: hreyesvivas@yahoo.com.mx or Gabriel López-Velázquez, Insurgentes Sur 3700-C, Col. Insurgentes Cuicuilco. México, D.F. CP 04530. E-mail: glv_1999@yahoo.com.

Received 9 December 2010; Revised 17 May 2011; Accepted 27 May 2011
Published online 16 June 2011 in Wiley Online Library (wileyonlinelibrary. com).
DOI: 10.1002/prot.23100

We have previously proposed that key enzymes, involved in the energetic metabolic pathways of *G. lamblia,* can be used as targets for drug design.[8,9] *G. lamblia* employs glycolysis as its main pathway for ATP production[10]; therefore, blocking this pathway could result in an energy deficit that might impair the survival of this parasite. Triosephosphate isomerase (TIM) has been considered as a potential target for drug design in several parasites.[11–13] It has been catalytically and structurally characterized in different organisms, including *Homo sapiens*[14] and human pathogens, such as *G. lamblia.*[8] Recently, we reported complete and selective inactivation of *G. lamblia* TIM (GlTIM) by chemical modification of Cys residues with thiol-reactive compounds (i.e., by the derivatization of these amino acid residues).[15] We found that the derivatization of at least one of the five Cys residues in GlTIM, presumably Cys222 or Cys228, was involved in the inactivation of the enzyme; however, the cysteine residue responsible for this inactivation could not be completely ascertained.

Inactivation of GlTIM is achieved by local structure perturbation without dimer dissociation, which suggests a possible communication between the region of the derivatized Cys that affects the activity and the catalytic site. The mechanism involved in this inactivation is quite different from that reported for TIMs of other species; in the latter, the derivatization of the interfacial Cys induces dissociation of the dimers and consequently, inactivation.[12,13,16]

In this study, experiments involving mutagenesis, enzyme kinetics, fluorescence, calorimetry, and protein structure were performed to precisely describe the mechanism of GlTIM inactivation by thiol reagents. The results of our mutagenesis studies indicate that Cys222 is the derivatization target that produces total enzyme inactivation. The kinetic and fluorescence experiments show that the inactivation of GlTIM achieved by Cys222 derivatization is caused by the perturbation of the affinity for the substrate. Additionally, isothermal calorimetric studies showed that derivatization of Cys222 mainly altered the entropic component for the binding of the ligand 2-phosphoglycolate (2-PG). Finally, the crystal structure of mutant C202A GlTIM derivatized with the thiol reagent methylmethane thiosulfonate (MMTS), was solved and confirmed that the Cys residues at positions 14, 222, and 228 were chemically modified, whereas the Cys127 was unaltered.

Our results describe a novel mechanism for the inactivation of GlTIM by chemical modification of a non-interfacial Cys residue and we also identified the region surrounding Cys222 as a suitable surface target for the design of molecular compounds with antigiardiasic activity of high specificity.

MATERIAL AND METHODS

General procedures

All reagents were of analytical grade. Protein concentrations were determined, either by the bicinchoninic acid method,[17] or by absorbance at 280 nm for pure GlTIM (ε_{280} = 26,600 M^{-1} cm^{-1}).[8] The enzymatic activity of GlTIM was measured in the direction of D-glyceraldehyde 3-phosphate (GAP) to dihydroxyacetone phosphate (DHAP) at 25°C, using a coupled spectrophotometric assay, by following the oxidation of NADH at 340 nm.[15] The standard reaction mixture contained 100 m*M* triethanolamine, 10 m*M* EDTA, pH 7.4, 1 m*M* GAP, 0.2 m*M* NADH, and 0.9 units of α-glycerol-3-phosphate dehydrogenase, and the assay was initiated by the addition of 5 ng of GlTIM per mL to the reaction mixture. For the determination of kinetic constants, GAP concentrations ranging from 0.4 to 3.5 m*M*, were used for the determination of the initial velocity and the data were adjusted to the Michaelis-Menten model using non-linear regression calculations. Recombinant His-tagged tobacco etch virus protease (TEVP) was expressed and purified as described by Rodríguez-Almazán *et al.*[18]

Site directed mutagenesis of GlTIM

Previously isolated *gltim* gene[8] was sub-cloned into a modified pET-3a plasmid (pET-HisTEVP), which introduced a $(His)_6$-tag and a tobacco etch virus protease recognition sequence at the amino-terminus of the protein (Supporting Information). Five desired Cys to Ala mutations, at positions 14, 127, 202, 222, and 228, were constructed by site directed mutagenesis.[19] The corresponding mutagenic oligonucleotides were as follows: C14A, Fwd: 5′-GTAACTTCAAGGCTAACGGC-3′ and Rev: 5′-GCCGTTAGCCTTGAAGTTAC-3′; C127A, Fwd: 5′-GGT CATCTTCGCTGTCGG-3′ and Rev: 5′-CCGACAGCGAA-GATGACC-3′; C202A, Fwd: 5′-GGAGAAGGTTGCTG CCG-3′, and Rev: 5′-CGGCAGCAACCTTCTCC-3′; C222A, Fwd: 5′-GGAAGCAACGCTGAGAAGC-3′, and Rev: 5′-GCTTCTCAGCGTTGCTTCC-3′; and C228A, Fwd: 5′-CC AGGCTCCGAATATTGAC-3′, and Rev: 5′-GTCAATATTCG GAGCCTGG-3′. Amplification conditions were reproduced as reported.[20] For all mutants, the wild-type gene was first cloned into the pET-HisTEVP plasmid and used as template. Successful mutagenesis was confirmed by DNA sequencing.

GlTIM expression and purification

Wild-type (WT) GlTIM or the mutants were expressed and purified following the same procedure. Cell culture and protein expression were performed as previously reported,[15] with some modifications. Briefly, BL21(DE3)-

Additional Supporting Information may be found in the online version of this article.
Grant sponsor: Consejo Nacional de Ciencia y Tecnología (CONACyT, México); Grant numbers: 104841, 62321 and 106126
*Correspondence to: .

pLysS cells containing the pET-HisTEVP-TIM plasmid (WT GlTIM or mutants) were grown at 37°C in LB medium plus 100 mg L^{-1} ampicillin until an OD_{600nm} of 0.6 was reached. Expression was induced overnight with 0.4 m*M* isopropyl β-D-galactopyranoside at 30°C. Protein purification was performed using immobilized metal-affinity chromatography (IMAC) with a Profinity Ni^{2+}-charged resin (Biorad). Transformed cells expressing $(His)_6$-tagged GlTIM were harvested by centrifugation and resuspended in lysis buffer containing 50 m*M* Tris (pH 8.0), 50 m*M* NaCl, 5 m*M* β-mercaptoethanol, 1 m*M* phenylmethylsulfonyl fluoride (PMSF), and 0.1% NaN_3. Cells were maintained at 4°C, disrupted by sonication and centrifuged at 9000 RPM for 30 min. The supernatant was added to the IMAC column, previously equilibrated with lysis buffer (without PMSF), and washed with 10 column volumes of the same buffer. Absorbed protein was eluted with lysis buffer containing 250 m*M* imidazole and concentrated to ~ 1 mL with Amicon Ultra filters (Millipore). The protein was precipitated with 75% saturated ammonium sulfate and centrifuged at 12,000 RPM and 4°C for 20 min. The supernatant was discarded and the pellet was suspended in 50 m*M* Tris (pH 8.0), 0.5 m*M* EDTA, and 1 m*M* dithiothreitol (TEVP buffer). To remove the His-tag from GlTIM, the enzyme was incubated for 17 h at room temperature with TEVP at a molar ratio of 30:1 (TIM:TEVP). Both the non-cleaved GlTIM and TEVP were removed by an additional IMAC step, performed using a batch modality. As indicated by SDS-PAGE analysis, the purity of the sample was higher than 95% and typical yields were ~ 50 mg per liter of culture. Proteins were stored in 100 m*M* triethanolamine and 10 m*M* EDTA, pH 7.4 (TE buffer). Alternatively, the proteins were precipitated with 75% saturated ammonium sulfate and maintained at 4°C until use.

Structural spectroscopic studies

Circular dichroism assays were performed using a Jasco J-810 spectropolarimeter, equipped with a Peltier-thermostated cell holder, in a cell with a path length of 0.1 cm. Spectral scans were carried out at 25°C, using a protein concentration of 100 μg mL^{-1}, with samples previously dialyzed against 25 m*M* phosphate at pH 7.4, and were performed at 1 nm intervals from 200 to 260 nm. To evaluate the thermal stability of WT GlTIM or the mutants, protein unfolding was measured as the change in the circular dichroism signal, at 222 nm, as a function of the temperature. The temperature scanning experiments were performed from 25°C to 70°C with an increase of 1°C min^{-1}. In all cases, the spectra of the samples without protein were subtracted from those that contained the enzyme. The fraction of apparent denatured protein was calculated as previously described.[15]

Fluorescence experiments were performed using a Perkin–Elmer LS55 spectrofluorometer at 25°C and a protein concentration of 500 μg mL^{-1}. The intrinsic fluorescence of the enzymes was determined at an excitation wavelength of 295 nm and the emission spectra was recorded from 310 to 500 nm using 13.2 and 3.6 nm excitation and emission slits, respectively. Each spectrum was the average of five scans. The spectra of blanks were subtracted from those containing protein.

Inactivation of GlTIM by chemical modification of cysteine residues

The sulfhydryl reagents methylmethane thiosulfonate (MMTS), 2-carboxyethyl methanethiosulfonate (MTSCE), and 5,5′-dithio-bis (2-nitrobenzoic acid) (DTNB) were prepared immediately before use. The WT GlTIM inactivation assays were performed at a protein concentration of 0.2 mg mL^{-1} (7.2 n*M*) in TE buffer at 25°C. Pseudo first-order inactivation rate constants were obtained at MTSCE concentrations ranging from 50 to 150 μ*M*, whereas the concentration for DTNB varied from 12.5 to 75 μ*M*. At the times indicated in Figure 1(A,B), aliquots were removed from the samples and assayed for residual activity in the standard reaction mixture. Data were adjusted to a monoexponential decay model,

$$A_R = A_0 e^{-kt} \quad (1)$$

where A_R is the residual activity at time t, A_0 is the activity at time 0, and k is the pseudo first-order inactivation rate constant. The second-order MTSCE inactivation rate constant was calculated from the slope of the linear plot of the pseudo first-order inactivation constant versus the concentration of MTSCE. For DTNB, the apparent second-order inactivation rate constant was calculated from the hyperbolic plot of the pseudo fist-order inactivation rate constant *versus* the concentration of DTNB. Data were adjusted to the equation $k = k_{MI} \times [DTNB]/K_{0.5} + [DTNB]$, where k_{MI} is the maximal inactivation rate constant achieved at DTNB saturation, whereas $K_{0.5}$ is the concentration of DTNB that gave 1/2 k_{MI}. The $k_{MI}/K_{0.5}$ ratio was considered as the apparent second-order inactivation rate constant. The number of free GlTIM cysteine residues was calculated as follows: 0.2 mg mL^{-1} of enzyme, WT GlTIM, or single cysteine mutants, were incubated at 25°C in TE buffer at the concentrations of sulfhydryl reagents indicated in Figure 1(C,D). After 2 h, aliquots were withdrawn from the samples and assayed for residual activity in the standard reaction mixture, and the free cysteine content was determined in the remaining sample according to the Ellman method, as previously reported.[15]

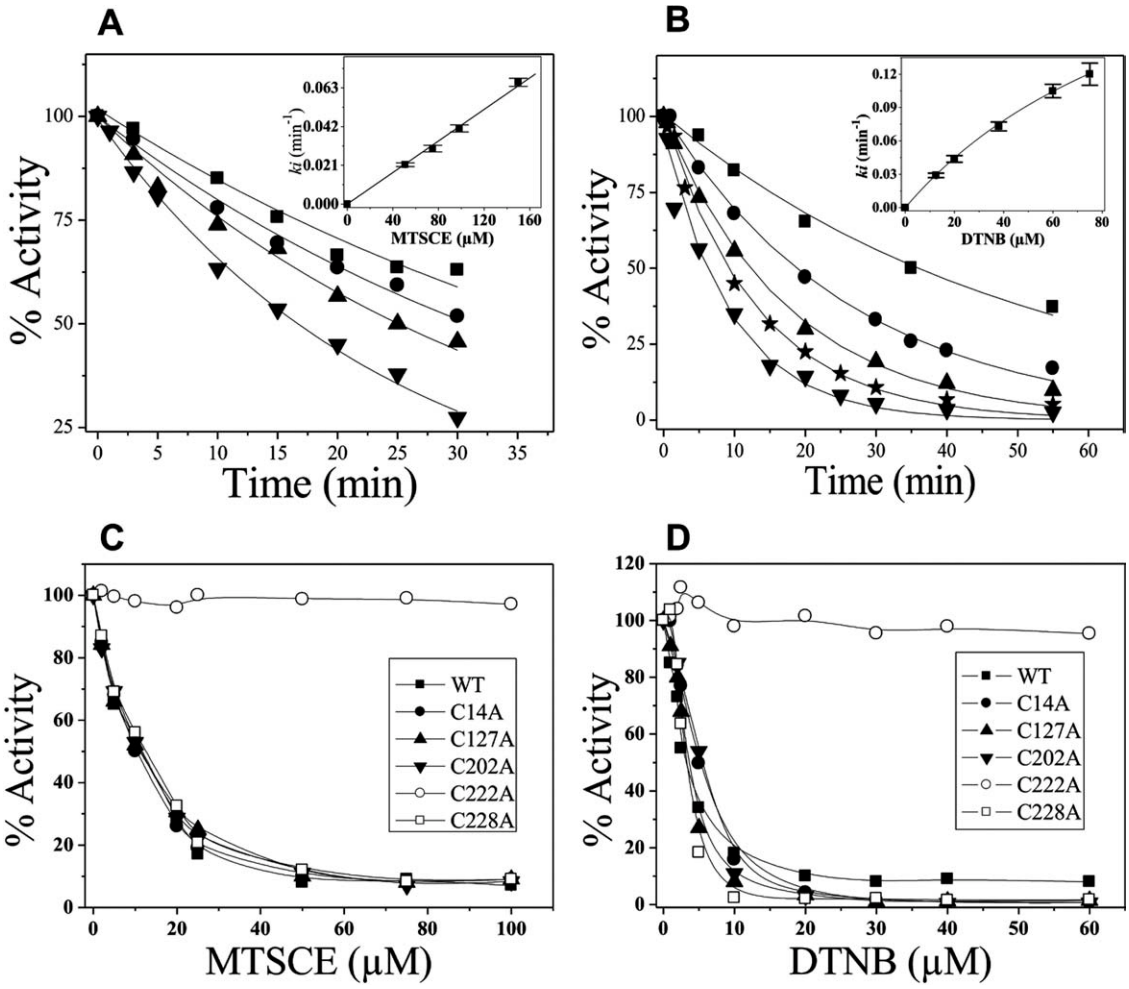

Figure 1

Inactivation of WT GlTIM or the single cysteine mutants by chemical modification of cysteine residues. WT GlTIM was incubated with 50 (■), 80 (●), 100 (▲), and 150 (▼) μ*M* MTSCE (**A**), or 12.5 (■), 20 (●), 38 (▲), 60 (★), and 75 (▼) μ*M* DTNB (**B**). At the indicated times, aliquots were withdrawn and assayed for residual activity; lines represent the fit of experimental data to Eq. (1). The insets show the replots of pseudo first-order inactivation rate constants versus the concentration of MTSCE (A) or DTNB (B). WT GlTIM (■) or single Cys mutants C14A (●), C127A (▲), C202A (▼), C222A (○), and C228A (□) were incubated at 25°C at the indicated concentrations of MTSCE (**C**) or DTNB (**D**). After 2 h, aliquots were withdrawn and assayed for residual activity. In both experiments, the enzymes were stable in the absence of sulfhydryl reagents during the incubation time.

Determination of the affinity of GlTIM for 2-PG

The change in intrinsic fluorescence of GlTIM, in response to the addition of 2-PG, was used to evaluate the affinity of modified or unmodified WT and the C222A mutant enzymes. We selected 2-PG because this is a well-studied transition-state analog with micromolar affinity for several TIMs.[21] Titrations of unmodified proteins were performed at concentrations ranging from 0.5 μ*M* to 1 m*M* by adding successive microliter aliquots of a concentrated 2-PG solution. The final volume added to the fluorescence cell was always <5% of the final volume. For the modified GlTIM, 1 mL of the WT or C222A mutant enzymes was incubated at 2 mg mL^{-1} for 2 h at 25°C with 5 m*M* MMTS or MTCSE. After this time, free sulfhydryl reagents were removed by column filtration (using 1 mL of Sephadex G-25 previously equilibrated in TE buffer). After elution, the protein concentration and the residual activity were determined, and titration with 2-PG was performed as indicated. The maximal fluorescence intensity of each spectrum at 332 nm was normalized and plotted *versus* the concentration of 2-PG. The ligand dissociation constant (K_D) was calculated by fitting the data to non-linear regression calculations with the equation

$$y = (\alpha/2E_t)[(E_t + x + K_D) - \sqrt{(E_t + x + K_D)^2 - 4xE_t}] \quad (2)$$

where $y = 1 - (F_i/F)$ (F_i, initial fluorescence; F, fluorescence intensity at each 2-PG concentration), α is the maximal fluorescence change attained at the saturating concentration of ligand, E_t represents the concentration of binding sites, and x is the concentration of 2-PG.[22] The free energy change of ligand binding was calculated from the fluorescence data [ΔG(flr)] using the values for K_D in the standard thermodynamic relation:

$$\Delta G(\text{flr}) = -RT\ln K_D \quad (3)$$

Isothermal titration calorimetry of 2-PG binding

The thermodynamic parameters of 2-PG binding to GlTIM were obtained by Isothermal Titration Calorimetry (ITC) using a high-precision iTC200 calorimeter (MicroCal). The assays were performed at 25°C with a protein concentration of 180 μ*M* in TE buffer. The 2-PG concentration in the syringe was 3.3 m*M*, and the titration schedule consisted of 20–30 consecutive 1 μL injections, with 2.4 min intervals between each application. To determine the heats of ligand dilution, experimental titrations were performed using buffer without protein in the reaction cell and the calculated values were subtracted from the experimental trace isotherm. The K_D, the enthalpy change (ΔH), and the binding stoichiometry (n) values were determined by non-linear fitting of the normalized titration data using a model with identical and independent binding sites.[23]

Crystallization, data collection, and structure determination of C202A GlTIM derivatized with MMTS

The C202A GlTIM was crystallized using the hanging drop vapor-diffusion technique at 18°C. The best crystals were obtained by mixing equal volumes of a protein solution at a concentration of 13.0 mg mL^{-1} in TE buffer and the precipitant solution, which contained 2*M* $(NH_4)_2SO_4$, 0.1*M* Tris-HCl, pH 8.5 (Hampton Research). Long, thick prisms with an orthorhombic I222 space group were obtained in 1 month. When the crystals reached a length of 0.7 mm, we began changing the mother liquor by extracting 0.5 μL and subsequently adding 0.5 μL of a solution with MMTS (20 m*M* MMTS in TE buffer); thus, the final MMTS concentration inside the drop was 1 m*M* after each application. Under these conditions, the hydrolysis rate constant of MMTS was 0.02 min^{-1}, with a half-life of 34.6 min (data not shown). The addition of MMTS to the crystal was repeated every day for 5 days, after which, diffraction data were collected.

The diffraction data from the C202A GlTIM crystals, soaked with MMTS, were obtained using a Raxis II-C image-plate detector mounted on a Rigaku rotating anode generator (Cu Kα, λ = 1.5416 Å) at 100 K. Diffraction images were processed and scaled using with XDS[24] and SCALA,[25] respectively. The summary of data collection and processing is given in Table III.

The monomeric structure in the asymmetric unit was solved by molecular replacement using the program Phaser[26] and the C202A GlTIM coordinates previously obtained (PDB entry code 2DP3). Refinement was conducted in Phenix[27] and model building and correction procedures were performed using COOT[28] and σA-weighted $2F_0-F_c$ and F_0-F_c maps. A test set that contained 10% of the reflections was reserved for cross-validation. Water molecules were added to the model near the end of refinement by a search procedure that is based on peaks observed in the difference maps and bond-distance criteria. PROCHECK[29] was used for the analysis of the model stereochemistry and validation. The figures were prepared with PyMOL.[30]

The atomic coordinates and structure factors have been deposited in the RSCB Protein Data Bank (PDB) with the accession number 3PF3.

Table I
Kinetic and Stability Constants of WT GlTIM and the Single Cysteine Mutants

GlTIM	K_m (m*M*)	k_{cat} (10^5 min^{-1})	k_{cat}/k_m (min^{-1} m*M*$^{-1}$)	Tm_{app} (°C)
WT[9]	0.78 ± 0.06	4.6 ± 0.16	5.9 × 10^5	57.5
C14A	0.4 ± 0.06	5 ± 0.16	12 × 10^5	55.1
C127A	0.36 ± 0.06	3.5 ± 0.1	9.7 × 10^5	52.6
C202A[8]	0.8 ± 0.09	2.9 ± 0.14	3.6 × 10^5	56.6
C222A[8]	1.8 ± 0.3	5 ± 0.4	2.8 × 10^5	58.6
C228A[8]	0.25 ± 0.07	1.87 ± 0.19	7.5 × 10^5	57.2

The kinetic constants were obtained for the reaction in the direction of GAP to DHAP. Initial velocity data at GAP concentrations ranging from 0.4 to 3.5 m*M* were fitted to the Michaelis-Menten equation and the k_{cat} per dimer is reported. The values are the average of three independent experiments (± standard errors). Tm_{app} values were obtained from circular dichroism temperature scan experiments from 25 to 70°C (1°C min^{-1}); the unfolding of proteins was monitored by the molar ellipticity change measured at 222 nm. The values are the average of two independent assays.

RESULTS

Kinetic parameters and thermal stability of GlTIM

Five point mutants, with an Ala replacing each Cys residue (C14A, C127A, C202A, C222A, and C228A), were constructed and their kinetic parameters were determined (Table I). The values of the K_m for mutants C14A, C127A, and C228A were one-half that of WT GlTIM, whereas for C222A GlTIM was two-fold higher; the k_{cat}

for C228A was also one-half that of the WT enzyme. There were no significant differences in all the other kinetic parameters. Circular dichroism spectra were recorded to evaluate the secondary structure of the enzymes (Supporting Information) and there were no significant differences between the WT enzyme and the mutants. Additionally, the stability of the mutants was determined following their thermal denaturation. With the exception of the C127A GlTIM, in which the Tm_{app} value decreased 5°C, the Tm_{app} of the rest of the mutants were similar to that of WT GlTIM, suggesting similar structural stabilities (Table I). Collectively, these data indicate that the overall structure of WT GlTIM and its mutants, are similar.

Inactivation of WT GlTIM and its mutants by thiol-reactive compounds

Previously, we showed that the derivatization of a non-interfacial Cys in GlTIM promotes subtle conformational changes that induce total enzyme inactivation, without perturbing the global 3D structure.[15] In this study, we evaluated the kinetics of enzyme inactivation produced by Cys derivatization with thiol-reactive compounds, to improve our understanding of the mechanism of GlTIM inactivation. The results show that the kinetics of inactivation using different concentrations of either MTSCE or DTNB, decays following a monoexponential function [Fig. 1(A,B), respectively]; however, the plots of the first-order rate constant versus thiol-reactive compound concentrations, showed different patterns. The data with MTSCE fit onto a straight-line with a second-order rate constant value of 7.1 ± 0.16 M^{-1} s^{-1} [Fig. 1(A), inset]. In contrast, the DTNB data fit onto a hyperbolic curve [Fig. 1(B), inset]. This behavior points to the presence of a reversible intermediary complex before the formation of the irreversibly inactivated enzyme.[31] Thus, an apparent second-order rate constant value of 43.4 ± 0.03 M^{-1} s^{-1} was calculated for DTNB, as described in the Material and Methods section.

We previously found that inactivation of GlTIM is mediated by derivatization of Cys222 or Cys228, or both; however, the Cys residue responsible for the inactivation remained undetermined.[15] We tested the susceptibility to inactivation with MTSCE or DTNB of the single Cys GlTIM mutants, to identify which Cys residues produce this inactivation [Fig. 1(C,D), respectively]. The results show that, in the presence of MTSCE, four mutants, C14A, C127A, C202A, and C228A exhibited a susceptibility similar to that of WT GlTIM [Fig. 1(C)]. Only the C222A GlTIM was completely resistant to the effects of MTSCE. The behavior of the mutants was similar when exposed to DNTB: only the C222A GlTIM remained completely resistant, but the rest of the GlTIM mutants lost their catalytic activities [Fig. 1(D)]. These data indicate that the derivatization of Cys222 is responsible for the inactivation of GlTIM.

To confirm the role of Cys222 as a unique target that promotes GlTIM inactivation, we determined the reactivity of the four remaining Cys residues in the C222A GlTIM. The results showed that after the enzyme was incubated with 100 μ*M* of MTSCE or DTNB for 2 h, the number of free Cys dropped to one per subunit, indicating that three Cys residues had been derivatized. These results led us to the conclusion that, although other Cys residues are modified chemically, it is the derivatization of Cys222 that is exclusively responsible for the total inactivation of GlTIM.

The derivatization of Cys222 decreases the affinity GlTIM for the substrate analog 2-PG

We previously evaluated the effect of derivatization of the Cys on the kinetic parameters of GlTIM. Although derivatization with MMTS increased the K_m two-fold, without modification of the k_{cat}, derivatization with MTSCE increased the K_m 10-fold and significantly decreased the k_{cat}.[15] Our data suggested that the thiol-reactive compounds affect the enzyme at two possible levels: substrate affinity and catalysis. To gain insight into the mechanism of the inactivation process, we evaluated the effect of Cys derivatization upon the binding of the substrate analog 2-PG, by following the changes of the intrinsic fluorescence signal of GlTIM in response to the addition of this ligand. Figure 2 shows that the fluorescence emission spectra from unmodified WT GlTIM was intensified as the 2-PG concentrations were increased, with a limit in the intensity change at ligand-saturating concentrations [Fig. 2(A)]. The emission spectra from WT GlTIM derivatized with MMTS showed a reduction in fluorescence intensity with respect to unmodified WT GlTIM; however, when the derivatized enzyme was exposed to different 2-PG concentrations, there was also an increase in the fluorescence intensity [Fig. 2(B)]. WT GlTIM derivatized with MTSCE exhibited a different behavior: it was exposed to different 2-PG concentrations and its intrinsic fluorescence intensity did not change [Fig. 2(C)].

Fluorescence emission spectra analyses were also performed using the C222A GlTIM. For all conditions, including those unmodified or modified with MMTS or MTSCE, the presence of 2-PG increased the fluorescence intensity of the enzyme [Fig. 2(E–G)]. It is noted that, the derivatization of the C222A GlTIM with MTSCE promoted a maximal fluorescence wavelength emission that had a red shift of 4 nm [Fig. 2(G)]; however, this effect was lost when the 2-PG concentration was increased in the experiments.

From these data, the maximal fluorescence intensity values for each spectrum was calculated, normalized, and

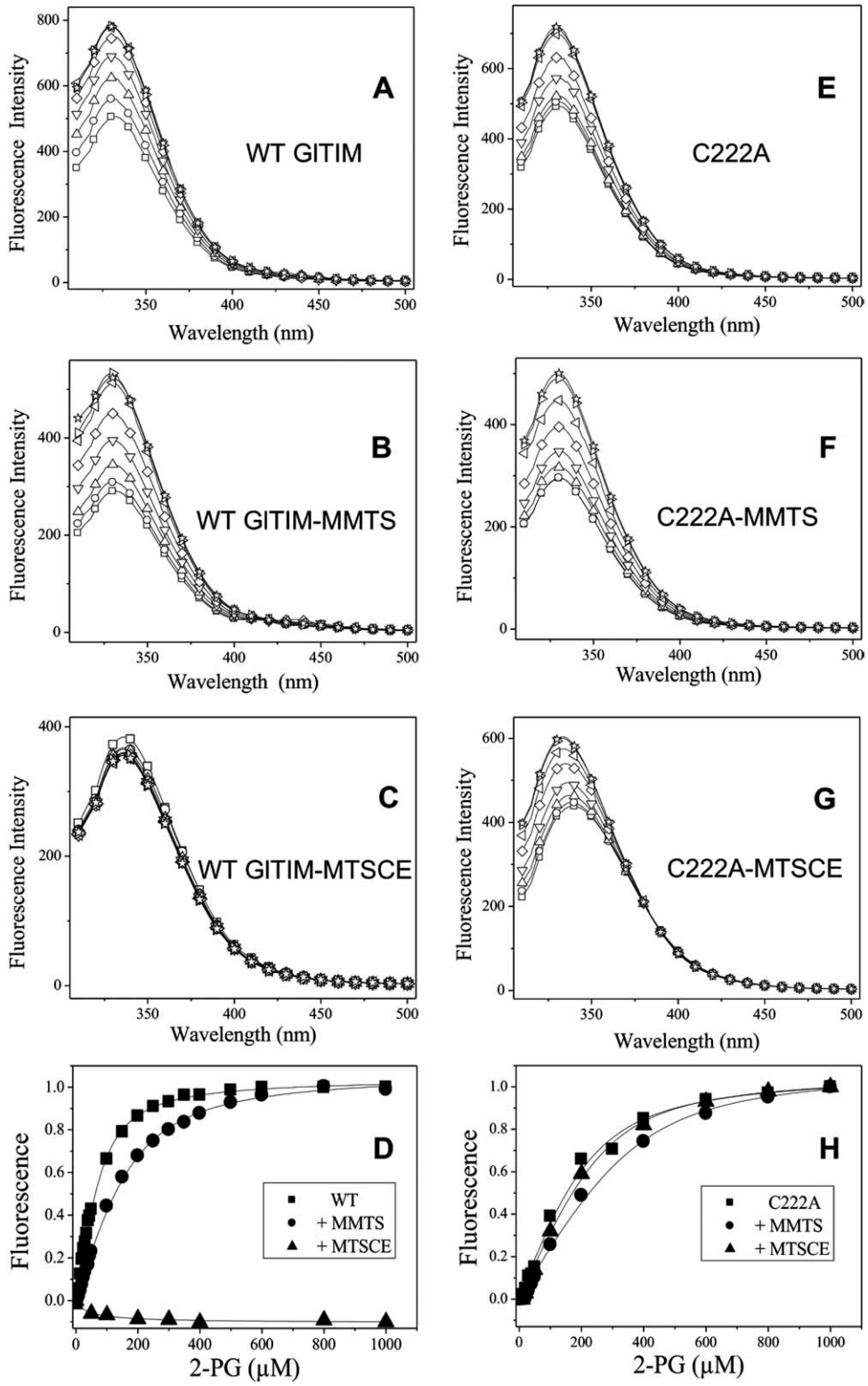

Figure 2

Fluorometric titration of 2-PG binding to WT GlTIM or to the C222A GlTIM. Fluorescence emission spectra of WT GlTIM (**A–C**) and the C222A GlTIM (**E–G**) in the unmodified, MMTS derivatized, and MTSCE derivatized forms of the enzymes. The experimental conditions are described in the Materials and Methods section. For clarity, only some of the representative concentrations of 2-PG were plotted: 0 μ*M* (□), 20 μ*M* (○), 50 μ*M* (△), 100 μ*M* (▽), 200 μ*M* (◇), 500 μ*M* (◁), 800 μ*M* (▷), and 1000 μ*M* (*). From these graphics, the maximal fluorescence intensity values were taken and plotted as a function of 2-PG concentration: WT GlTIM (**D**) or the C222A GlTIM (**H**) illustrate the unmodified (■), MMTS derivatized (●), and MTSCE derivatized (▲) forms of the enzymes.

Table II
Fluorometric and Calorimetric Parameters for 2-PG Binding to Unmodified and MMTS Derivatized WT GlTIM

WT GlTIM	No. of sites	K_D(flr) (μM)	K_D(cal) (μM)	ΔH (cal) (kcal mol^{-1})	$-T\Delta S$ (cal) (kcal mol^{-1})	ΔG (flr) (kcal mol^{-1})	ΔG (cal) (kcal mol^{-1})
−MMTS	0.91 ± 0.04	26.4 ± 2.6	53	−7.41 ± 0.15	1.48	−6.3	−5.93
+MMTS	0.9 ± 0.01	57.8 ± 4.7	80	−9.2 ± 0.23	3.6	−5.86	−5.6

The K_D values obtained from the fluorescence experiments (flr) were calculated from the data in Figure 2 and fitted by non-linear regression according to Eq. (2). ΔG(flr) was calculated using the K_D values according to Eq. (3). The thermodynamic parameters (cal) were calculated as previously described.[21] The values are the average of two independent experiments (± standard errors).

plotted against the concentration of 2-PG. Figure 2(D) confirms that the derivatization of WT GlTIM with MMTS induced a curve shift towards higher concentrations of 2-PG when compared with the plot of the unmodified WT GlTIM. When the intensities of WT GlTIM derivatized with MTSCE were plotted as a function of the concentration of 2-PG, it was found that the change in fluorescence signal was abolished. These data indicate that Cys derivatization with thiol-reactive compounds, in particular MTSCE, decreased the affinity of WT GlTIM for its ligand.

A plot of maximal fluorescence intensities as a function of the concentration of 2-PG was also performed with the data for the C222A GlTIM [Fig. 2(H)]. As expected, the graphs clearly showed that the mutant conserved the affinity for 2-PG, even when the enzyme was previously derivatized with both MMTS and MTSCE. Thus, these data confirm that the derivatization of Cys222 in GlTIM is exclusively responsible for the decrease in the affinity for the ligand.

The values of the K_D for the GlTIM-2PG complex were calculated from the data in Figure 2 (Table II). While the K_D for the unmodified WT GlTIM correlates with the value reported by kinetic approaches (∼ 25 μM),[21] the K_D of the derivatized WT GlTIM with MMTS was two-fold higher. The K_D value of the enzyme derivatized with MTSCE was not determined because the changes in intrinsic fluorescence were lost. The K_D was

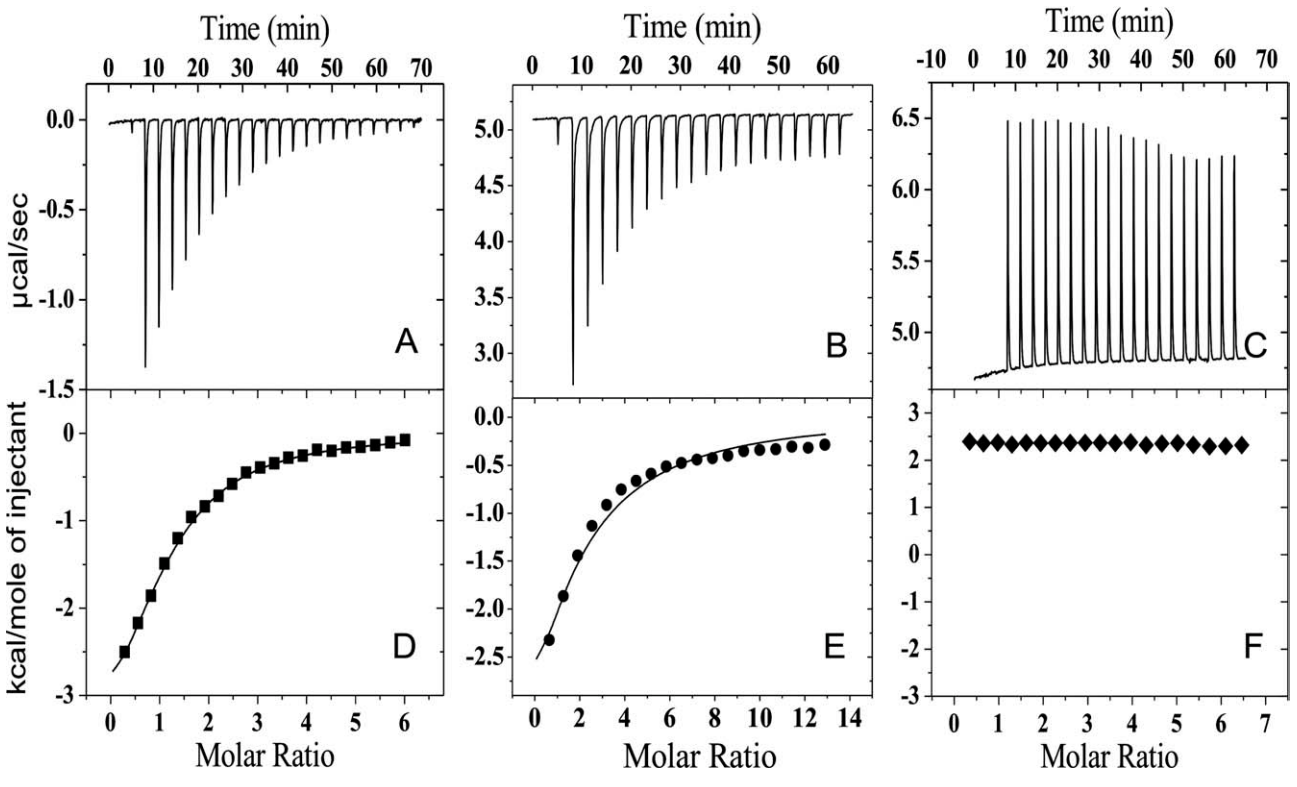

Figure 3
Isothermal titration calorimetry for the binding of 2-PG to WT GlTIM. Thermograms of 2-PG binding to the unmodified (**A**), MMTS derivatized (**B**), or MTSCE derivatized (**C**) forms of enzyme. In all conditions, the final enzyme concentration was 4 mg mL^{-1}. Isothermal titration obtained from the thermograms of unmodified (**D**), MMTS derivatized (**E**), or MTSCE derivatized enzymes (**F**). The heat dilution was subtracted in all cases and the data were fitted to a one ligand per subunit model.[22]

52 μ*M* for the C222A GlTIM and was twice that of WT GlTIM; such a decrease in affinity correlates with the change in the K_m value for GAP (Table I). The values for the K_D of the C222A GlTIM, treated with either MMTS or MTSCE, respectively were 1.3- and 1.2-fold higher, when compared to the unmodified C222A GlTIM. Thus, despite having three derivatized Cys residues, the affinity of the modified C222A GlTIM for 2-PG did not change significantly.

Calorimetric 2-PG binding parameters of WT GlTIM

To obtain further insight into the effect of derivatizing Cys on the affinity of GlTIM for 2-PG, the thermodynamic parameters of 2-PG binding to WT GlTIM, and derivatized WT GlTIM, were explored using ITC. Figure 3(A) shows that the reaction of 2-PG binding to WT GlTIM is exothermic. The change in the heat recorded in the thermogram decreased as the 2-PG concentration progressively increased in the reaction cell. Figure 3(D) shows the isothermal binding after subtracting the dilution heat. In this case, the solid line corresponds to a model with a best-fit that relates to the binding of one ligand per acceptor subunit. When WT GlTIM was derivatized with MMTS, the binding of 2-PG to the enzyme was also exothermic [Fig. 3(B)]. The isothermal binding also fitted well to the model of one ligand per subunit [Fig. 3(E)]. In contrast, successive injections of 2-PG into WT GlTIM derivatized with MTSCE did not promote detectable heat changes in the ITC instrument [Fig. 3(C,F)]. This indicates that the derivatization of WT GlTIM with MTSCE induces a total loss in ligand affinity. Hence, taking the kinetic, calorimetric and the intrinsic fluorescence data together, it is clear that the derivatization of Cys222 by a negatively charged bulky thiol compound like MTSCE (or DTNB), induces a drastic perturbation of the binding affinity of WT GlTIM for its substrates.

Table II summarizes the thermodynamic parameters obtained from fits of the isothermal binding data. The K_D value obtained by ITC for the unmodified WT GlTIM was two-fold higher than the value obtained by fluorometric titration, and the K_D value obtained by ITC for the derivatized enzyme with MMTS was 1.4-fold higher than the value obtained by fluorescence. Such differences between calorimetric and fluorometric data have also been observed in studies of yeast TIM[22] and may be due to the higher concentrations of both GlTIM and 2-PG, used during the calorimetric experiments, a condition that may induce the loss of an ideal binding interaction.

The binding reaction of 2-PG with WT GlTIM, in both the unmodified and MMTS derivatized enzymes, produced a negative ΔH at 25°C. In addition, the $T\Delta S$ value was 2.4-fold higher in derivatized WT GlTIM. The addition of 2-PG to the derivatized enzyme with MTSCE did not promote a change in heat; consequently, its thermodynamic analysis could not be performed. Taking the data together, it suggests that the loss of affinity induced by derivatization could be due to local perturbations of the structure that surrounds Cys222 and not to global conformational changes in GlTIM.

Table III
Data Collection and Structure Refinement Statistics for MMTS-C202A GlTIM

Data collection	
Space group	I222
Cell dimensions (Å)	a = 56.37
	b = 102.88
	c = 118.91
Unique reflections[a]	22,165 (1297)
Resolution limit (Å)	50.2–2.1
R^b_{merge}	0.051 (0.26)
Multiplicity	3.0 (2.9)
Completeness (%)	96.7 (90.8)
I/σ (I)	9.8 (2.8)
Refinement statistics	
R^c/R_{free} (%)	18.35/21.1
No. of atoms of	
Protein/solvent/	2011/129
Glycerol/sulfate/Ca	30/10/1
Average B value (Å^2)	32.38
RMSD from ideality	
Bond length (Å)	0.009
Bond angle (°)	1.042
Ramachandran plot (%)	
Allowed regions	99.1
Disallowed	0.9

[a]Values in parentheses correspond to the last resolution shell.
[b]$R_{merge} = \sum_j \sum_h (|I_{j,h} - \langle I_h \rangle|)/\sum_j \sum_h (\langle I_h \rangle)$, where h is the unique reflection index, $I_{j,h}$ is the intensity of the symmetry-related reflection, and $\langle I_h \rangle$ is the mean intensity.
[c]$R = \sum_h || F_0|_h - |F_c|_h|/\sum_h |F_0|_h$ for all reflections, where F_0 and F_c are observed and calculated structure factors, respectively, and h defines unique reflections. R_{free} was calculated similarly to the test reflections, randomly selected, and excluded from the refinement.

Overall structure of the MMTS adduct of C202A GlTIM

To investigate possible conformational changes induced by Cys derivatization that affect ligand binding, we attempted to obtain the structure of GlTIM derivatized with the thiol-reactive compounds. We used the C202A GlTIM for the crystallographic studies because this mutant exclusively forms a dimeric species[8] that yields a homogeneous sample and rapid crystallization of the enzyme. After obtaining the enzyme crystals, they were soaked in solutions containing MMTS, MTSCE or DTNB to derivatize their Cys residues. The soaking of crystals in solutions of MTSCE or DTNB induced crystal cracking in a few hours; therefore, they were not appropriate for data collection. In contrast, a crystal soaked with MMTS was able to diffract, allowing us to solve the structure of the modified enzyme at a resolution of 2.2 Å. The data-collection and refinement statistics are shown in Table

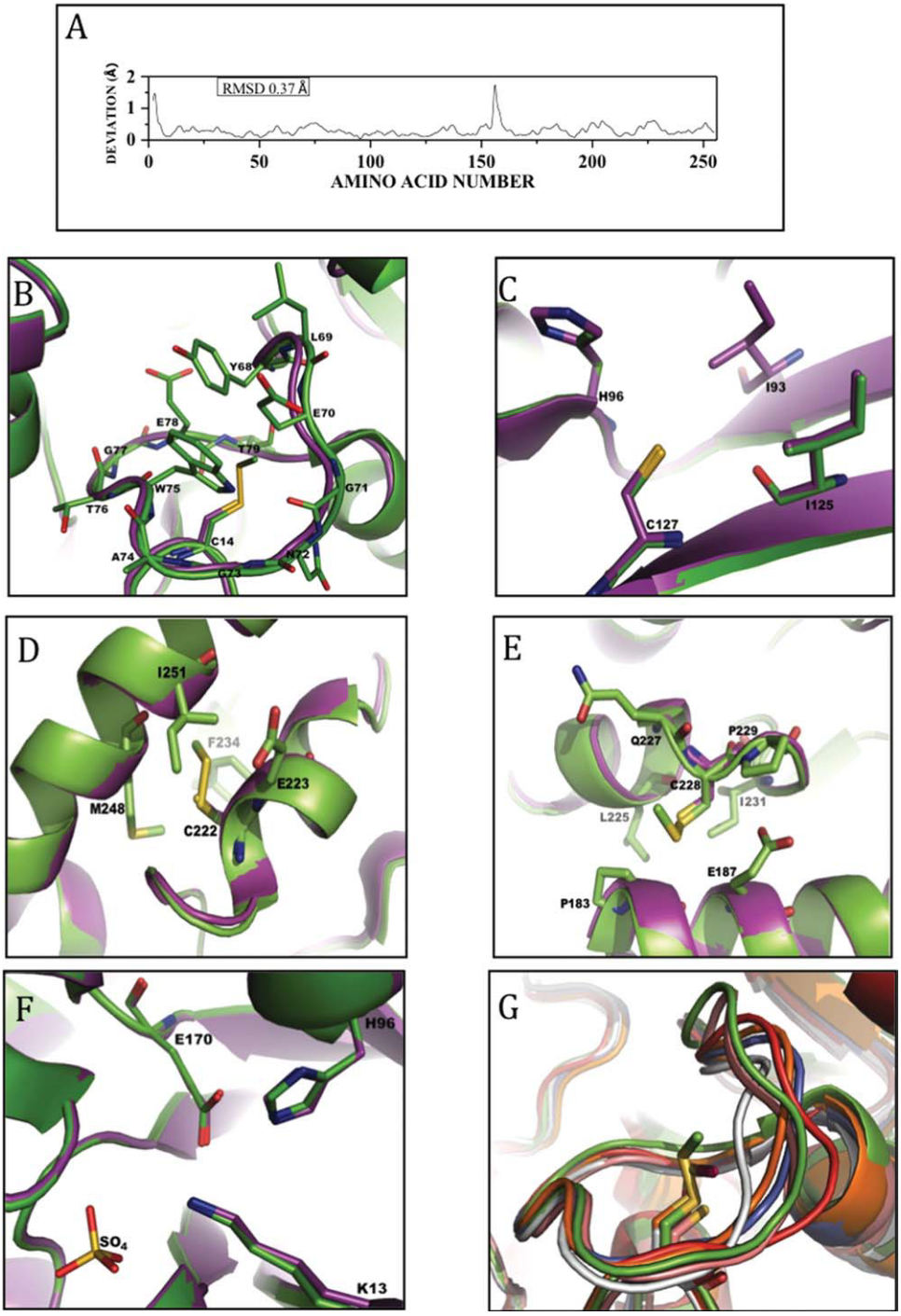

Figure 4

Structure of the MMTS-C202A GlTIM. Measurement of the deviation from the C^{α} distances between the C202A GlTIM (2DP3) and the MMTS-C202A GlTIM (3PF3) after the optimal superposition of all equivalent C^{α} pairs[43] (**A**). Ribbon representation of the neighborhoods at 5 Å of Cys14 (**B**), Cys127 (**C**), Cys222 (**D**), and Cys228 (**E**) from the structures of the C202A GlTIM (violet) and the MMTS-C202A GlTIM (green). A close-up of the catalytic site from the C202A GlTIM (violet) and the MMTS-C202A GlTIM (green) structures (**F**). Superposition of Loop 3 region from the MMTS-C202A GlTIM (green), TbTIM (blue), TcTIM (orange), EhTIM (gray), PfTIM (brown), and HuTIM (red) (**G**). The side chains are represented as sticks. The figures were prepared using the PyMOL program.[30]

III. The structure of the MMTS-C202A GlTIM (3PF3) closely resembles that of WT GlTIM (2DP3), with a maximal value of RMS deviation for the Cα atoms of 0.37 Å [Fig. 4(A)].

Table IV
Properties of the Cavity Region in Loop 3 Containing the Interfacial Cys Residues for TIMs of Several Different Parasites

Protein	PDB code	Volume (Å^3)	Number of residues of Loop 3	Effect of interfacial Cys derivatization with MMTS	Ref.
C202A GlTIM	2DP3	94.7	16	No dissociation/No inactivation	8,15
MMTS-C202A GlTIM	3PF3	122.7	16	No dissociation/No inactivation	15 and this study
PfTIM	1YDV	97.2	16	N.D.	13
EhTIM	1M6J	76.9	15	Dissociation/Inactivation	12
LmTIM	1AMK	74.4	15	Dissociation/Inactivation	39,44
TbTIM	5TIM	68.3	15	Dissociation/Inactivation	40,44
TcTIM	1TCD	68	15	Dissociation/Inactivation	41,44

The cavity volumes in the Loop 3 were generated *in silico* by removing the B subunit of TIM and using the A subunit in all cases. The CASTp server (Computed Atlas of Surface Topography of Proteins) was used to calculate the volume values of the cavities.[42]

The structure of the MMTS-C202A GlTIM showed that the Cys residue at position 14 clearly displayed an additional electron density corresponding to a thioalkyl group [i.e., —S—CH_3; Fig. 4(B)]. Electron density maps showed only one conformation for Cys14; therefore, the thioalkyl group is bound with full occupancy (data not shown). The thioalkyl was oriented toward the region of the residues Tyr68, Leu69, and Glu70 in Loop 3 of the adjacent subunit. Interestingly, it appears that this region creates a space to accommodate the thioalkyl group without clashes [Fig. 4(B)]. The overlap of Loop 3 between the structures of the unmodified and derivatized enzymes did not allow a clear identification of conformational changes induced by the thioalkyl group. However, when we determined the dimension of the cavity formed inside the Loop 3 (Asn66 to Ser80), after the adjacent monomer had been removed *in silico*,[32] the cavity volume in the unmodified enzyme amounted to 94.7 Å^3, while this value was increased to 122.7 Å^3 in the MMTS-C202A GlTIM (Table IV). Hence, the introduction of a thioalkyl group on the sulfur atom of Cys14 generated a distortion of the interfacial loop.

Respect to Cys127, the electron density for the thioalkyl group over the sulfur atom was absent [Fig. 4(C)]; even considering that, for crystallization conditions, the C202A GlTIM was exposed for 35 min to MMTS concentrations ranging from 1 to 0.5 m*M* during five days. An explanation for this result may be that Cys127 reacts poorly with thiol-reactive compounds; consequently, the MMTS concentrations to which the crystal of enzyme was exposed were insufficient for derivatization. These results correlate with our previous biochemical data indicating that, of the five Cys residues present in each subunit of WT GlTIM, one was not available for derivatization by thiol-reactive compounds.[15]

The thioalkyl Cys residue at position 222 was located in a hydrophobic pocket [Fig. 4(D)], whereas the thioalkyl group on Cys228 was oriented toward the solvent [Fig. 4(E)]. The overlap of unmodified GlTIM and the MMTS-C202A GlTIM surprisingly showed that there were no significant conformational rearrangements in any of the Cys residues. Likewise, there were no appreciable conformational differences between the catalytic sites of either structure [Fig. 4(F)]. Additionally, a sulfate molecule was found in the phosphate-binding site of the structure of the MMTS-C202A GlTIM and Loop 6 was found in the closed conformation. The sulfate interactions detected in this structure are equivalent to those observed in the crystal structure of the *Trypanosoma brucei* TIM (TbTIM) with sulfate.[32,33]

DISCUSSION

The GlTIM Cys222 is a specific target for drug design

This study describes the Cys222 residue of GlTIM as a novel target for the inactivation of this parasite enzyme. The proposal of Cys222 as a target is supported by three main points: (i) The derivatization of Cys222 with MTSCE or DTNB induces complete enzyme inactivation, (ii) the inactivation assays with the single Cys mutants indicated that C222A GlTIM was completely resistant to inactivation, even though three of its four Cys residues were derivatized [Fig. 1(C,D)], and (iii) the assays with HuTIM indicated that it is 200-fold less reactive to thiol-reactive compounds than GlTIM. This last point is especially relevant, since HuTIM also has a Cys residue in the equivalent position of Cys222 in GlTIM.[15]

Although TIM has been previously proposed as a plausible target for rational drug design, the specific target region proposed in this report has not been described in the TIMs from other parasites. For instance, the interfacial Cys residues in TbTIM, *T. cruzi* TIM (TcTIM), *Leishmania mexicana* (LmTIM),[16] *Entamoeba histolytica* TIM (EhTIM),[12] and *Plasmodium falciparum* TIM (PfTIM)[13] have been proposed as targets, since their derivatization induces total enzyme inactivation. GlTIM also has the interfacial Cys; however, its derivatization did not induce inactivation.[15]

The mechanism of inactivation of GlTIM by derivatization of Cys222 involves ligand binding perturbation

The analysis of the titration of the reaction of 2-PG with GlTIM using fluorometry indicated that the derivatization of Cys222 significantly decreased the affinity for the ligand [Fig. 2(D)]. The level of affinity perturbation seems to correlate with the size and polarity of the thiol-reactive compounds, that is: MMTS, a small and neutral compound, increased the K_D two-fold, whereas MTSCE, a bulky and negative compound, completely prevented the binding of 2-PG to the enzyme. The data from the ITC confirm these results: the derivatization of Cys222 with MMTS induced minor perturbations on the energy of the binding reaction. The ΔG(cal) values of untreated and derivatized WT GlTIM were -5.93 kcal mol^{-1} and -5.6 kcal mol^{-1}, respectively. In addition, we observed that its entropy value was 2.43-fold higher than that for unmodified WT GlTIM (Table II). This increase could be attributed to two general reasons: (i) perturbation of weak intermolecular interactions that decrease the order in the ligand binding region[34] inducing an increase in the value of the K_D or (ii) perturbation of the properties of the structural water molecules in the derivatized WT GlTIM. Further analyses are needed to clarify the origin of such differences. For the experiments of derivatization with MTSCE, the determination of thermodynamic parameters was not achieved because the binding of 2-PG to the enzyme was totally abolished.

To compare the reactivity of GlTIM with the reactivity of TIMs from other parasites, using a thiol-reactive compound, we compared the rate constants of inactivation by derivatization with DTNB. The value of the second-order rate constant for GlTIM is 1.8-fold higher than the value for TcTIM and 290-fold higher than the value for TbTIM.[36] In addition, the kinetics of inactivation of GlTIM with DTNB showed a hyperbolic behavior, indicating that the region surrounding Cys222 operates as a recognition site that initially binds to DTNB, prior to reacting covalently with the Cys. Hence, Cys222 shows the highest reactivity with thiol-reactive compounds, and selectivity in the binding to distinct molecules.

Structural data of the MMTS-C202A GlTIM

The derivatization of the C202A GlTIM with MMTS did not show any apparent conformational changes in the regions surrounding Cys222 and Cys228. Because the biochemical data of the derivatization of Cys222 showed that MMTS reduced the k_{cat} value by half[15] and produced a two-fold increase in the K_D value for 2-PG (Table II), it was reasonable to expect some conformational changes in the region surrounding this residue, and around the catalytic site. In this regard, it has been previously reported that the presence of ligands in the catalytic sites of TbTIM and TcTIM, affect the reactivity of their interfacial Cys residues to thiol-reactive compounds.[35] The second-order rate constants for the derivatization of their interfacial Cys are diminished in the presence of 2-PG.[36] This suggests that occupancy of the catalytic site may promote an increase in the structural stability of TIM, which protects it from derivatization. In this context, the C202A GlTIM was crystallized in the presence of 2*M* ammonium sulfate, which has been identified as a ligand for TIMs in other species, with a K_i value of around 5 m*M*.[37] Hence, the generation of contacts between the sulfate molecule and the catalytic pocket of the MMTS-C202A GlTIM may produce the stabilization of this region and the preservation of its catalytically competent conformation. Consequently, conformational perturbations are not observed. Attempts are currently being performed to make crystals of the MMTS-C202A GlTIM in the absence of ligands.

Although the crystal structure did not provide insight into the molecular mechanism of inactivation by the derivatization of Cys222, it was instructive to analyze the derivatized Cys14. The thioalkyl group of this residue fits inside Loop 3, and induces subtle local perturbations without enzyme inactivation.[15] As previously mentioned, this interfacial Cys has been identified as a potential target for TbTIM, TcTIM, and EhTIM,[12,13,16] and their derivatization with MMTS induces dimer dissociation and total inactivation. Thus, a logical question that arises is: Why is GlTIM not inactivated or dissociated,[15] (this study) as a result of Cys14 derivatization with MMTS or MTSCE? The crystal structure shows that the Cys14 thioalkyl moiety (i.e., —S—CH_3, equivalent to 35 Å^3) is oriented toward the hydrophobic pocket of Loop 3 from the adjacent subunit that surrounds this Cys [Fig. 4(B)]. No steric hindrance or clashes were observed inside this region; however, the analysis of a virtual cavity formed inside Loop 3, when the adjacent subunit is removed, showed that the volume of this hole increased by 28 Å^3 (Table IV). Hence, it seems that the Loop 3 of GlTIM exhibits enough conformational flexibility to accommodate the thioalkyl, or even the thiocarboxyethyl moiety (62 Å^3) from MTSCE, without dimer dissociation. The ability of Loop 3 to accommodate Cys14 adducts of distinct sizes is probably provided by an additional residue in GlTIM: Asn 72, which makes this region longer than those observed in TbTIM, TcTIM, and EhTIM [Table IV and Fig. 4(G)]. Moreover, there is a clear correlation between the length of Loop 3, the cavity volume, and the derivatization effect of the interfacial Cys. The TIMs for which MMTS promotes dissociation and complete inactivation all have a Loop 3 region with 15 residues and the volume of their cavities ranges between 68 and 77 Å^3. In contrast, Loop 3 of GlTIM has 16 residues and a cavity volume of 95 Å^3, where derivatization of Cys14 with MMTS did not induce dissociation[15] or inactivation [Table IV and Fig. 4(G)]. Loop 3 of PfTIM also has 16 residues and a cavity volume of 97 Å^3 and, although there

are no data of derivatization with MMTS, the effect of amino acid substitutions of its interfacial Cys were recently reported.[38] Two PfTIM mutants, C13D and C13E, respectively, showed a 7.4-fold and 3.3-fold decrease in their k_{cat}; however, they were able to retain their dimeric structure at protein concentrations above of 1.25 μM.[38] Hence, it seems that Loop 3 of PfTIM also has the capacity to accommodate extra volumes. Finally, HuTIM naturally has a Met instead of a Cys in the interfacial region [Fig. 4(G)], adding an extra volume of 38 $Å^3$ and its Loop 3 also contains 16 residues with a cavity volume of 130 $Å^3$ (PDB code 2JK2). This enzyme exhibits very high dimer stability.[18]

CONCLUDING REMARKS

In conclusion, this study describes a novel mechanism for GlTIM inactivation that involves the perturbation of the substrate affinity as a consequence of the derivatization of Cys222, which is distant from the catalytic site. The structural environment that surrounds this residue has unique structural properties that can be exploited as a candidate surface target for designing highly specific antigiardiasic compounds with low adverse effects for the host. Docking studies are now in progress to obtain lead molecules that can bind with high specificity to the region surrounding Cys222.

ACKNOWLEDGMENTS

S.E.F. was the recipient of a fellowship from CONACyT. This work is part of the Ph.D. thesis of S.E.F. for the Posgrado en Ciencias Biológicas, Universidad Nacional Autónoma de México. The authors thank Dr. Ruy Perez-Montfort for careful revision of the manuscript.

REFERENCES

1. Thompson RC. Giardiasis as re-emerging infectious disease and its zoonotic potential. Int J Parasitol 2000;30:1259–1267.
2. Müller N, von Allmen N. Recent insights into the mucosal reactions associated with *Giardia lamblia* infections. Int J Parasitol 2005;35: 1339–1347.
3. Upcroft JA, Dunn LA, Wright JM, Benakli K, Upcroft P, Vanelle P. 5-Nitroimidazole drugs effective against metronidazole-resistant *Trichomonas vaginalis* and *Giardia duodenalis*. Antimicrob Agents Chemother 2006;50:344–347.
4. Lindmark DG, Muller M. Antitrichomnad action, mutagenecity, and reduction of metronidazole and other nitroimidazoles. Antimicrob Agents Chemother 1976;10:476–482.
5. Argüello-García R, Cruz-Soto M, Romero-Montoya L, Ortega-Pierres G. Variability and variation in drug susceptibility among *Giardia duodenalis* isolates and clones exposed to 5-nitroimidazoles and benzimidazoles *in vitro*. J Antimicrob Chemother 2004;54:711–721.
6. Suk DH, Rejman D, Dykstra CC, Pohl R, Pankiewicz KW, Patterson SE. Phosphonoxins: rational design and discovery of a potent nucleotide anti-Giardia agent. Bioorg Med Chem Lett 2007;17:2811–2816.
7. Torres-Gómez H, Hernández-Núñez E, León-Rivera I, Guerrero-Alvarez J, Cedillo-Rivera R, Moo-Puc R, Argotte-Ramos R, Rodríguez-Gutiérrez Mdel C, Chan-Bacab MJ, Navarrete-Vázquez G. Design, synthesis and in vitro antiprotozoal activity of benzimidazole-pentamidine hybrids. Bioorg Med Chem Lett 2008;18:3147–3151.
8. Reyes-Vivas H, Diaz A, Peon J, Mendoza-Hernandez G, Hernandez-Alcantara G, De la Mora-De la Mora I, Enriquez-Flores S, Dominguez-Ramirez L, Lopez-Velazquez G. Disulfide bridges in the mesophilic triosephosphate isomerase from *Giardia lamblia* are related to oligomerization and activity. J Mol Biol 2007;365:752–763.
9. López-Velázquez G, Molina-Ortiz D, Cabrera N, Hernández-Alcántara G, Peon-Peralta J, Yépez-Mulia L, Pérez-Montfort R, Reyes-Vivas H. An unusual triosephosphate isomerase from the early divergent Eukaryote *Giardia lamblia*. Proteins 2004;55:824–834.
10. Schofiel PJ, Edwards MR, Kranz P. Glucose metabolism in *Giardia intestinalis*. Mol Biochem Parasitol 1991;45:39–47.
11. Ostoa-Saloma P, Garza-Ramos G, Ramírez J, Becker I, Berzunza M, Landa A, Gómez-Puyou A, Tuena de Gómez-Puyou, Pérez-Montfort R. Cloning, expression, purification and characterization of triosephosphate isomerase from *Trypanosoma cruzi*. Eur J Biochem 1997;244:700–705.
12. Rodríguez-Romero A, Hernández-Santoyo A, del Pozo Yauner L, Kornhauser A, Fernández-Velasco DA. Structure and inactivation of triosephosphate isomerase from *Entamoeba histolytica*. J Mol Biol 2002;322:669–675.
13. Velanker SS, Ray SS, Gokhale RS, Suma S, Balaram H, Baralam P, Murthy MR. Triosephosphate isomerase from *Plasmodium falciparum*: the crystal structure provides insights into antimalarial drug design. Structure 1997;5:751–761.
14. Mande SC, Mainfroid V, Kalk KH, Goraj K, Martial JA, Hol WG. Crystal structure of recombinant human triosephosphate isomerase at 2.8 Å resolution. Triosephosphate isomerase-related human genetic disorders and comparison with the trypanosomal enzyme. Protein Sci 1994;3:810–821.
15. Enriquez-Flores S, Rodriguez-Romero A, Hernandez-Alcantara G, De la Mora-De la Mora I, Gutierrez-Castrellon P, Carvajal K, Lopez-Velazquez G, Reyes-Vivas H. Species-specific inhibition of *Giardia lamblia* triosephosphate isomerase by localized perturbation of the homodimer. Mol Biochem Parasitol 2008;157:179–186.
16. Gao XG, Garza-Ramos G, Saavedra-Lira E, Cabrera N, De Gómez-Puyou MT, Perez-Montfort R, Gómez-Puyou A. Reactivation of triosephosphate isomerase from three trypanosomatids and human: effect of suramin. Biochem J 1998;332:91–96.
17. Smith PK, Krohn RI, Hermanson GT, Mallia AK, Gartner FH, Provenzano MD, Fujimoto EK, Goeke NM, Olson BJ, Klenk DC. Measurement of protein using bicinchoninic acid. Anal Biochem 1985;150:76–85.
18. Rodríguez-Almazán C, Arreola R, Rodríguez-Larrea D, Aguirre-López B, de Gómez-Puyou MT, Pérez-Montfort R, Costas M, Gómez Poyou A, Torres-Larios A. Structural basis of triosephosphate isomerase deficiency: mutation E104D is related to alterations of a conserved water network at the dimer interface. J Biol Chem 2008;283:23254–23263.
19. Ho SN, Hunt HD, Horton RM, Pullen JK, Pease LR. Site-Directed mutagenesis by overlap extension using the polymerase chain reaction. Gene 1989;77:51–59.
20. Hernández-Alcántara G, Rodríguez-Romero A, Reyes-Vivas H, Peon J, Cabrera N, Ortiz C, Enríquez-Flores S, De la Mora-De la Mora I, López-Velázquez G. Unraveling the mechanisms of tryptophan fluorescence quenching in the triosephosphate isomerase from *Giardia lamblia*. Biochim Biophys Acta 2008;1784:1493–1500.
21. Hartman FC, LaMuraglia GM, Tomozawa Y, Wolfenden R. The influence of pH on the interaction of inhibitors with triosephosphate isomerase and determination of the pKa of the active-site carboxyl group. Biochemistry 1975;14:5274–5279.
22. González-Mondragón E, Zubillaga RA, Saavedra E, Chánez-Cárdenas ME, Pérez-Montfort R, Hernández-Arana A. Conserved cysteine 126 in triosephosphate isomerase is required not for enzymatic activity

but for proper folding and stability. Biochemistry 2004;43:3255–3263.
23. Wiseman T, Williston S, Brandts JF, Lin LN. Rapid measurement of binding constants and heats of binding using a new titration calorimeter. Anal Biochem 1989;179:131–137.
24. Kabsch W. Automatic processing of rotation diffraction data from crystals of initially unknown symmetry and cell constants. J Appl Cryst 1993;26:795–800.
25. Collaborative Computational Project Number 4. The CCP4 suite: programs for protein crystallography. Acta Crystallogr D Biol Crystallogr 1994;50:760–763.
26. McCoy AJ, Grosse-Kunstleve RW, Adams PD, Winn MD, Storoni LC, Read RJ. Phaser crystallographic software. J Appl Crystallogr 2007;40:658–674.
27. Adams PD, Afonine PV, Bunkóczi G, Chen VB, Davis IW, Echols N, Headd JJ, Hung LW, Kapral GJ, Grosse-Kunstleve RW, McCoy AJ, Moriarty NW, Oeffner R, Read RJ, Richardson DC, Richardson JS, Terwilliger TC, Zwart PH. PHENIX: a comprehensive Python-based system for macromolecular structure solution. Acta Crystallogr D Biol Crystallogr 2010;66:213–221.
28. Emsley P, Cowtan K. Coot: model-building tools for molecular graphics. Acta Crystallogr D Biol Crystallogr 2004;60:2126–2132.
29. Laskowski RA, MacArthur MW, Moss DS, Thornton JM. PROCHECK: a program to check the stereochemical quality of protein structures. J Appl Crystallog 1993;26:283–291.
30. DeLano WL. The PyMOL molecular graphics system. Palo Alto, CA: DeLano Scientific; 2002. Available at: http://www.pymol.org.
31. Cardemil E. Kinetics of the chemical modification of enzymes. In: Eyzaguirre J, editor. Chemical modification of enzymes: active site studies. New York: John Wiley and Sons; 1987. pp 23–34.
32. Noble ME, Verlinde CL, Groendijk H, Kalk KH, Wierenga RK, Hol WG. Crystallographic and molecular modeling studies on trypanosomal triosephosphate isomerase: a critical assessment of the predicted and observed structures of the complex with 2-phosphoglycerate. J Med Chem 1991;34:2709–2718.
33. Noble ME, Wierenga RK, Lambeir AM, Opperdoes FR, Thunnissen AM, Kalk KH, Groendijk H, Hol WG. The adaptability of the active site of trypanosomal triosephosphate isomerase as observed in the crystal structures of three different complexes. Proteins 1991;10:50–69.
34. Dunitz JD. Win some, lose some: enthalpy-entropy compensation in weak intermolecular interactions. Chem Biol 1995;2:709–712.
35. Pérez-Montfort R, Garza-Ramos G, Alcántara GH, Reyes-Vivas H, Gao XG, Maldonado E, de Gómez-Puyou MT, Gómez-Puyou A. Derivatization of the interface cysteine of triosephosphate isomerasa from *Trypanosoma brucei* and *Trypanosoma cruzi* as probe of the interrelationship between the catalytic sites and the dimmer interface. Biochemistry 1999;38:4114–4120.
36. Reyes-Vivas H, Hernández-Alcantara G, López-Velazquez G, Cabrera N, Pérez-Montfort R, de Gómez-Puyou MT, Gómez-Puyou A. Factors that control the reactivity of the interface cysteine of triosephosphate isomerasa from *Trypanosoma brucei* and *Trypanosoma cruzi*. Biochemistry 2001;40:3134–3140.
37. Lambeir AM, Opperdoes FR, Wierenga RK. Kinetic properties of triose-phosphate isomerase from *Trypanosoma brucei brucei*. A comparison with the rabbit muscle and yeast enzymes. Eur J Biochem 1987;168:69–74.
38. Banerjee M, Balaram H, Joshi NV, Balaram P. Engineered dimer interface mutants of triosephosphate isomerase: role of inter-subunit interactions in enzyme function and stability. Protein Eng Des Sel 2011;24:463–472.
39. Williams JC, Zeelen JP, Neubauer G, Vriend G, Backmann J, Michels PA, Lambeir AM, Wierenga RK. Structural and mutagenesis studies of leishmania triosephosphate isomerasa: a point mutation can convert a mesophilic enzyme into superstable enzyme without losing catalytic power. Protein Eng 1999;12:243–250.
40. Wierenga RK, Noble ME, Vriend G, Nauche S, Hol WG. Refined 1.83 Å structure of trypnosomal triosephosphate isomerase crystallized in the presence of 2.4 M-ammonium sulphate. A comparison with the structure of the trypanosomal triosephosphate isomerase-glycerol-3-phosphate complex. J Mol Biol 1991;220:995–1015.
41. Maldonado E, Soriano-García M, Moreno A, Cabrera N, Garza-Ramos G, de Gómez-Puyou M, Gómez-Puyou A, Pérez-Montfort R. Differences in the intersubunit contacts in triosephosphate isomerase from two closely related pathogenic trypanosomes. J Mol Biol 1998;283:193–203.
42. Dundas J, Ouyang Z, Tseng J, Binkowski A, Turpaz Y, Liang J. CASTp: computed atlas of surface topography of proteins with structural and topographical mapping of functionally annotated residues. Nucleic Acids Res 2006;34:W116–W118.
43. Russell RB, Barton GJ. Multiple protein sequence alignment from tertiary structure comparison: assignment of global and residue confidence levels. Proteins 1992;14:309–323.
44. Garza-Ramos G, Cabrera N, Saavedra-Lira E, Tuena de Gómez-Puyou M, Ostoa-Saloma P, Pérez-Montfort R, Gómez-Puyou A. Sulfhydryl reagents susceptibility in proteins with high sequence similarity-triosephosphate isomerase from *Trypanosoma brucei*, *Trypanosima cruzi* and *Leishmania mexicana*. Eur J Biochem 1998; 253:684–691.
45. Stols L, Gu M, Dieckman L, Raffen R, Collart FR, Donnelly MI. A new vector for high-throughput, ligation-independent cloning encoding a tobacco etch virus protease cleavage site. Protein Expr Purif 2002;25:8–15.